

On the Use of a Well Stirred Reactor to Study Soot Inception

Samuel L. Manzello^{1*}, George W. Mulholland¹, Michael Donovan², and Wing Tsang²

¹Building and Fire Research Laboratory (BFRL)

²Chemical Science and Technology Laboratory (CSTL)

National Institute of Standards and Technology (NIST)

Gaithersburg, MD USA

Kihong Park and Michael R. Zachariah

Department of Mechanical Engineering and Chemistry

University of Maryland-College Park

College Park, MD USA

Scott D. Stouffer

University of Dayton Research Institute (UDRI)

Dayton, OH USA

ABSTRACT

A well stirred reactor (WSR) followed by a plug flow reactor (PFR) is being used to study polycyclic aromatic hydrocarbon (PAH) growth and soot inception. Soot size distributions were measured using a dilution probe followed by a nano-differential mobility analyzer (Nano-DMA). A rapid insertion probe was fabricated to thermophoretically collect particles from the reactor for transmission electron microscopy (TEM) analysis. Results are presented on the: (1) effect on the equivalence ratio of the soot size distributions obtained from the Nano-DMA for fixed dilution ratio (2) effect of dilution ratio on the soot size distributions obtained from the Nano-DMA for fixed equivalence ratio, and (3) comparison of soot size distributions obtained from the rapid insertion/TEM analysis and the Nano-DMA. The particle sizing results from the Nano-DMA and the rapid insertion/TEM analyses suggested that condensation of low vapor pressure species was occurring during the dilution process. Our size distribution measurements demonstrate that the mixing conditions in the flame zone affect whether or not a nucleation mode was detected in the size distribution.

INTRODUCTION

Soot is a common by-product resulting from the combustion of fossil fuels. Release of soot into the atmosphere by combustion processes contributes to environmental and health hazards. Sooting can also decrease the efficiency of combustion processes since carbonaceous particulates represent incomplete combustion and can lead to hardware fouling. On the other hand, soot formation is desirable in certain applications such as industrial furnaces since the presence of soot greatly enhances radiative heat transfer. The challenge is to be able to control soot formation for a specific task. This requires a detailed understanding of the soot formation process.

Unfortunately, understanding the mechanisms responsible for soot formation remains a daunting task. The major steps in soot formation consist of fuel pyrolysis, PAH formation, particle inception, coagulation, surface growth, carbonization, agglomeration, and oxidation [1-3]. The process of soot inception is the least understood aspect of soot formation.

It has long been recognized that a WSR coupled with a PFR has many advantages for soot inception studies compared to laminar flames. Understanding the chemistry of particle formation in laminar flames is difficult due to: (1) large concentration gradients (2) poor spatial resolution, and (3) the fact that the sampling methods disturb the flame [4]. The advantages of sampling particles from the PFR section are: (1) the gas velocity is large, so axial diffusion of species is negligible (2) the total residence time is spread over the entire length, so excellent spatial resolution is possible (3) disturbance due to sampling probes is minimal as a PFR does not have flame stability issues, and (4) the nearly isothermal conditions exist in the PFR [4].

To advance the understanding of soot inception in combustion systems requires detailed measurements of soot particle size distributions under conditions of incipient particle formation. Such measurements are needed to validate models of soot formation in flames. However, measuring the soot particle size distribution is not trivial because the particle size distribution must be maintained as particles are cooled and diluted. The goal of this study was to measure soot particle size distributions in a WSR/PFR using a diluter coupled with Nano-DMA. A diluter was used to minimize both coagulation growth of the particles and thermophoretic deposition on the sampling tube. The dilution probe described here allowed for

* Corresponding author: Office +1-301-975-6891 Fax +1-301-975-4052 email: samuel.manzello@nist.gov

dilution ratios of up to 10^4 , which are considerably larger than previously reported measurements in a WSR/PFR [5]. In addition, a rapid insertion probe was fabricated to thermophoretically collect particles from the reactor for transmission electron microscopy (TEM) analysis. Results are presented on the: (1) effect on the equivalence ratio of the soot size distributions obtained from the Nano-DMA for fixed dilution ratio (2) effect of dilution ratio on the soot size distributions obtained from the Nano-DMA for fixed equivalence ratio, and (3) comparison of soot size distributions obtained from the rapid insertion/TEM analysis and the Nano-DMA.

EXPERIMENTAL DESCRIPTION

Figure 1 (a) displays the NIST WSR/PFR. The reactor was comprised of four parts: (1) WSR (2) PFR (3) afterburner, and (4) cooling section. The WSR used premixed fuel and air, and exhibited both macroscopic and microscopic mixing during combustion, and approximated a highly turbulent combustion environment. The WSR, originally developed in 1955 [6], has been used extensively to study PAH and soot [4]. The NIST reactor was based on the design currently implemented by Stouffer *et al.* [7]. A cross section of the WSR, including the jet ring is shown in Figure 1 (b). The WSR consisted of a 250-ml toroidal chamber made of an upper and lower section of silicon carbide (SiC). An inconel jet ring was located in between the two SiC sections. Premixed fuel and air entered the WSR through 48 jets (1 mm diameter) at near sonic velocity. These jets caused rapid mixing of reactants, intermediates, and products within the WSR. The WSR was housed inside a steel casing and was followed by a PFR. Air and gaseous fuel flow rates were controlled using mass flow controllers. The air system for the WSR can accommodate flow rates up to 400 SLPM with pre-heat temperatures up to 420 K. Fuel cylinders were manifolded to provide a steady flow of up to 75 SLPM. The residence time in the WSR can be varied between 5 ms and 12 ms.

The exhaust gases from the WSR entered the PFR section through a flow straightener. The PFR section was 70 cm long and had an inner diameter of 5.1 cm. The PFR section included an inner silicon carbide insulating sleeve and an outer alumina section. The velocity of the gases in the PFR section was on the order of 10-20 m/s, thus total PFR residence times were on the order of 30 ms. The PFR section contained four sampling ports. In the present study, all sampling was performed in the bottommost port of the PFR section.

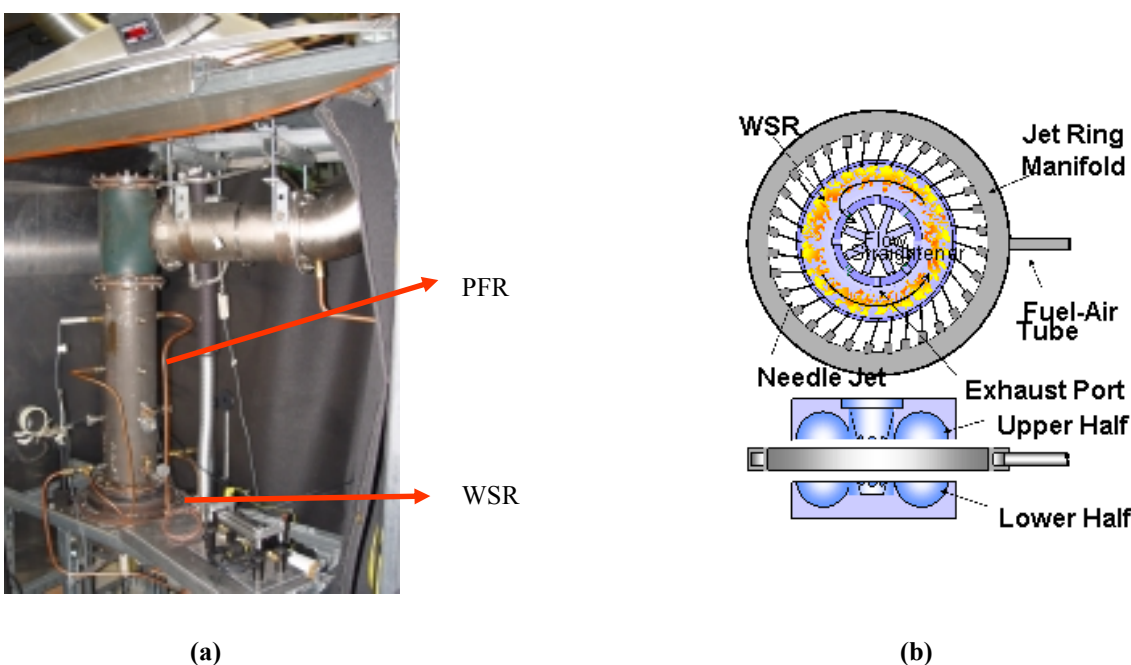


Fig. 1 (a) Picture of NIST WSR (b) Detail of the WSR section.

The fuel rich conditions necessary for soot inception resulted in volume fractions of CO in excess of 15 %. This is a serious safety issue. An afterburner was installed after the PFR section to burn out most of the CO. The afterburner consisted of an inconel 601 tube fitted with slits for air to pass through. During operation, air was introduced into the inconel 601 tube and the CO/air mixture auto-ignited. The CO/air flame was stabilized since the inconel 601 tube was designed to act as a bluff body. The final products were cooled using a water spray prior to being released to the ambient.

A dilution probe, based upon the design of Zhao *et al.* [8], was inserted into the PFR section. A schematic of the diluter is shown in figure 2. The dilution probe included a hypodermic tube (6.05 mm OD, 5.03 mm ID) with a single 0.50 mm orifice in the side wall for sampling the particulate and other combustion products. The flow of nitrogen entered through

one side of the tube and exited the other side of the probe (Figure 2). An ejector pump was used to adjust the pressure drop across the orifice to vary the dilution ratio from 10^2 to 10^4 . A portion of the diluted flow was sampled by a CO monitor to determine the dilution ratio. The undiluted CO concentration in the exhaust was estimated by computing the equilibrium distribution of products for specified temperatures. Nominal volume fractions were 16.5 % for $\Phi = 1.9$, $T = 1620$ K, 17.6 % at $\Phi = 2.0$, $T = 1580$ K, and 18.5 % at $\Phi = 2.1$, $T = 1540$ K. The probe was supported by a ceramic (zirconia) sleeve material which served to insulate the probe from the flow and from exhaust stack heat conduction. A section of the tube with a gap of 9.5 mm, which was also the OD of the sleeves, was exposed to the flow. This section was partially covered with a ceramic paste to help reduce the temperature of the capillary tube.

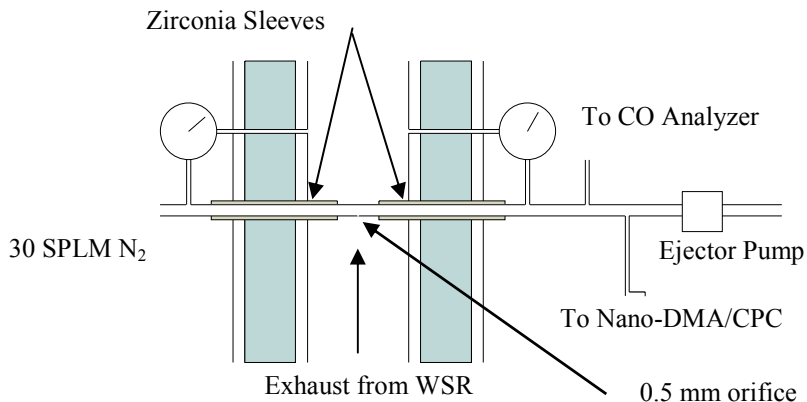


Fig. 2 Schematic of diluter installed in PFR.

The particle size distributions were measured downstream of the diluter by a Nano-Differential Mobility Analyzer (Nano-DMA). The concentration of the monodisperse aerosol leaving the Nano-DMA was monitored with a condensation nucleus counter (CPC). Nano-DMA voltage was maintained constant for 10 s with the CPC count data taken at the end of this interval. Typically data were collected at 30 voltages. Initially the rapid scanning procedure was used, but there were problems with lack of repeatability between the upward and downward scans.

A rapid insertion probe was fabricated to thermophoretically collect particles from the reactor for transmission electron microscopy (TEM) analysis (see figure 3). The probe assembly was pneumatic and was controlled using a pulse generator coupled to a solid state relay. The 3 mm diameter TEM grid was held in place by a miniature fork-shaped assembly contacting the TEM grid at its periphery. The pneumatically driven device (Figure 3) collected soot for 0.5 s. The probe remained in a N_2 purged tube until the pneumatic system was activated.

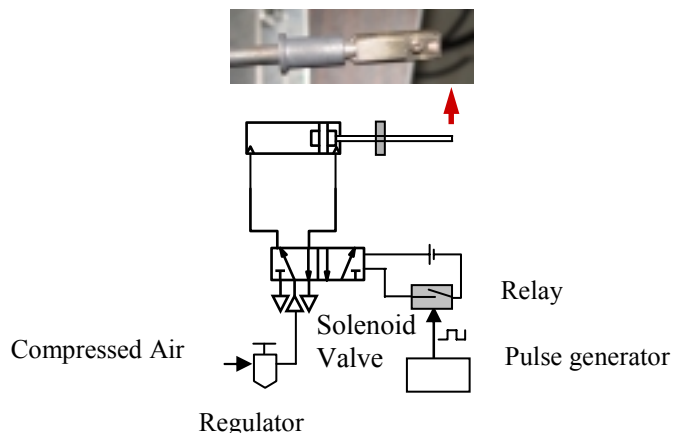


Fig. 3 Schematic of rapid insertion probe used to collect soot on TEM grids.

For the present experiments, ethylene (ultra high purity) was used as the fuel. The air flow rate was kept constant at 175 SLPM and the ethylene fuel flow rate was varied. Under these flow conditions, the residence time in the WSR was ~ 11 ms. Data was collected for four equivalence ratios near the soot inception point, namely $\phi = 1.8, 1.9, 2.0,$ and 2.1 . An hour of operation was required to reach a steady WSR/PFR temperature.

RESULTS AND DISCUSSION

The size distribution results are plotted in Figure 4 for four values of the equivalence ratio. At $\Phi = 1.8$, there was no indication of flame generated particles. The actual particle concentration obtained by the CPC for this condition was less than 1 particle/cm³ and the nominal value of 10⁵ cm⁻³ for the size distribution function was primarily a result of the 1000 fold dilution and the low charging probability of nanometer size particles. The peak in the size distribution at $\Phi = 1.9$ was a couple orders of magnitude larger than the background, but also a couple of orders of magnitude less than the values observed at the higher equivalence ratios. The peak in the size distribution at $\Phi = 1.9$ occurred at a particle size of 7 nm to 8 nm compared to 15 nm to 16 nm for $\Phi = 2.0$, and a broad peak extending from about 15 nm to 22 nm for $\Phi = 2.1$. The size distribution at $\Phi = 2.1$ was significantly broader than the other two. The large “jumps” in the size distribution occurred as the concentration increased from about 10 particles/cm³ to 100 particles/cm³ for the diluted smoke. This may be an artifact of the CPC counter for rapid changes in concentration at relatively low concentrations. The integrated results for the total number concentration and the mass concentration based on a soot density of 1800 kg/m³ are presented in Table 1 for the data of Figure 4.

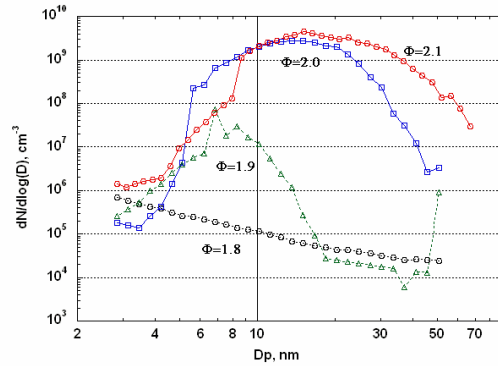


Figure 4. The size distributions obtained with the Nano-DMA are plotted for the WSR operating at four equivalence ratios close to the point of soot inception.

Equivalence Ratio	Number Concentration, #/cm ³	Mass Concentration, mg/m ³
1.9	1.8×10^7	0.009
2.0	2.7×10^9	11
2.1	4.2×10^9	49

Table 1. Integrated values of size distribution for data in figure 4.

Repeat measurements at $\Phi = 2.0$ agreed to within 2 nm to 3 nm for the location of the peak diameter at about 15 nm and to within about a factor of two for the size distribution functions (Figure 5). Size distribution measurements were made for dilution ratios of about 10³ and 10⁴. As demonstrated in Figure 5, the size distributions were not affected by the increased dilution. If coagulation were taking place during the dilution process, the size distribution of the more concentrated smoke would be shifted to larger particle sizes.

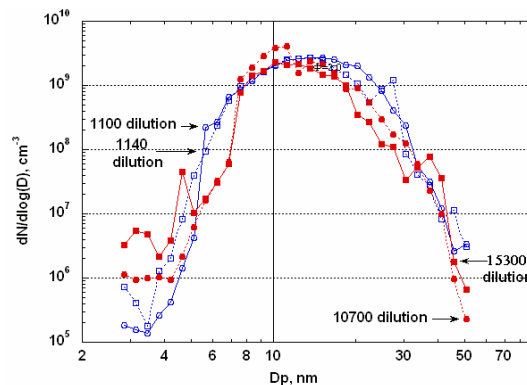


Figure 5. The effect of changing the dilution rate by about a factor of 10 for an equivalence ratio of 2.0 on the size distribution, which is plotted for the undiluted smoke in all cases.

In this study the particles were sampled using the rapid insertion probe at the same height as the dilution probe. The Nano-DMA size distribution was measured just before and after the TEM collection. The collection time for one insertion was about 0.5 s. Multiple insertions were required to obtain a high enough particle density to determine the size distribution. The minimum desired coverage was 10 particles per field of view for a magnification of 200,000. For $\Phi = 2.0$ and 2.1, ten insertions were adequate to obtain more than 10 particles per field over a large fraction of the grid.

At $\Phi = 1.9$, no particles were detected on the TEM grid, which was viewed at multiple locations. One possible explanation of this observation is that the concentration of smoke was so low that there were not enough particles collected to be detected. This explanation is consistent with the 100 fold lower particle concentration measured by the Nano-DMA at $\Phi = 1.9$ compared to values obtained for the larger equivalence ratios. A repeat experiment was performed and the number of insertions increased to 20 and 60. No particles were detected at 20 insertions, but at 60 insertions particles were detected at a few locations on the grid and the size distribution was determined. About 150 particles were measured to obtain each size distribution. Details of the analysis procedure are available elsewhere [9].

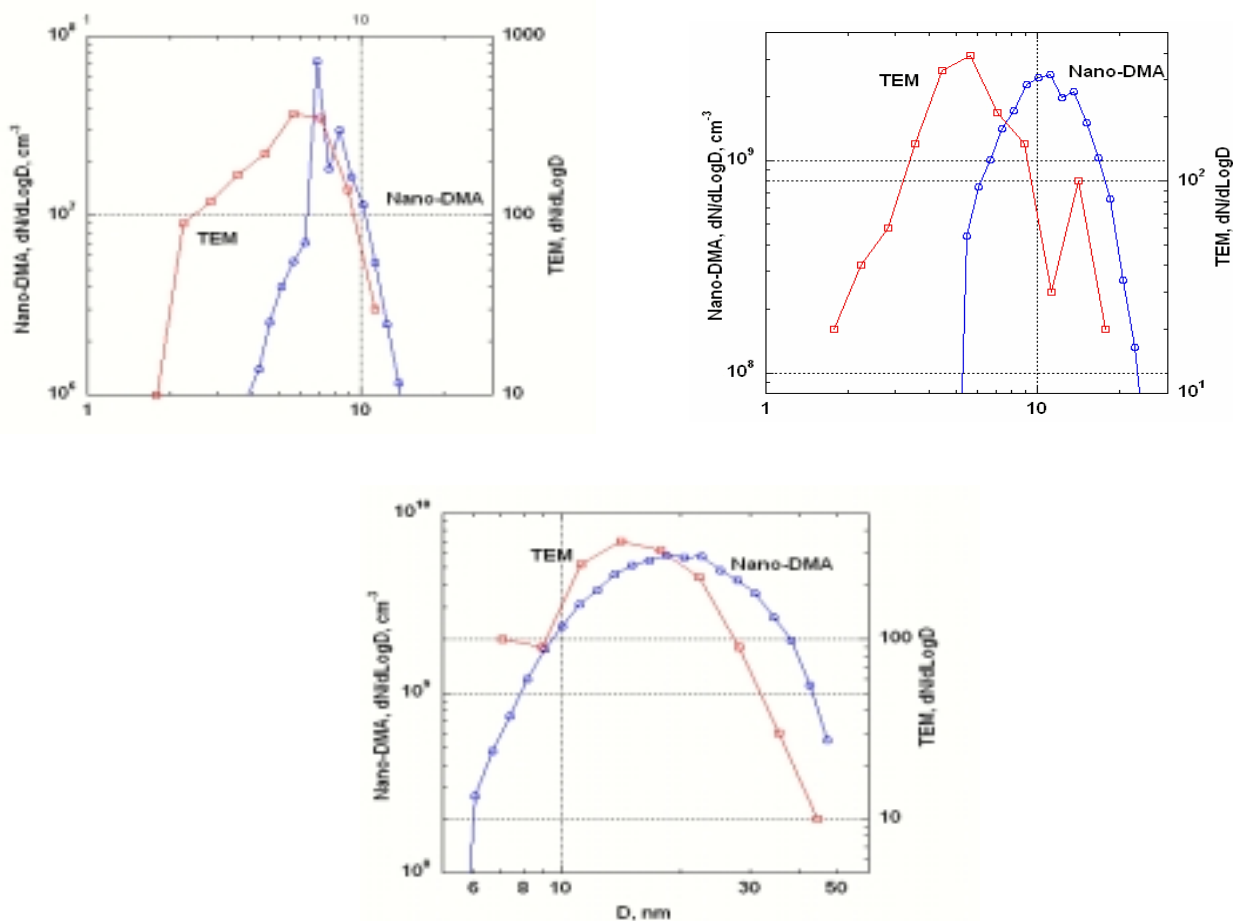


Figure 6. Comparison of the size distribution obtained by the nano-DMA and by TEM analysis. Top left, $\Phi=1.9$, top right $\Phi=2.0$, bottom, $\Phi=2.1$.

The size distribution obtained by the TEM analysis and the Nano-DMA analysis are compared in Figure 6. For $\Phi = 2.1$, the two size distributions were similar. The TEM distribution was narrower and had a smaller peak size of about 15 nm compared to about 20 nm for the Nano-DMA. For the other two equivalence ratios, the TEM results have a much larger fraction of particles at smaller sizes. This was especially apparent for $\Phi = 2$, where the peak size by TEM was about 6 nm compared to about 11 nm by the Nano-DMA. There are several possible explanations for this difference. The most likely explanation is that condensation of low vapor pressure PAHs and other hydrocarbons was taking place during the dilution process. If the vapor pressure of these species was low enough, the dilution will not decrease the amount of condensation growth per particle occurring as the temperature was decreased to ambient. Other possibilities include sampling losses for the Nano-DMA, the TEM microscope calibration for such small amorphous particle, and the effect of the low vacuum and the electron beam energy on reducing the particle size in the TEM.

Maricq [10] and Zhao *et al.* [11] reported size distribution measurements for soot collected from a pre-mixed ethylene-air flame generated by a 6 cm diameter, water cooled, McKenna burner. The authors used a Nano-DMA similar to the one here and a high dilution probe, also similar to the one reported presently. The size distribution obtained by Maricq [10] for $\Phi = 2.06$ had a peak at the smallest size measured, independent of the sampling height. This was qualitatively different from our findings. The reason for the difference may be the different combustion environment for a WSR compared to a premixed burner. In the WSR, the incoming fuel and air are rapidly mixed with the products of combustion including incipient soot, CO, PAHs, and free radicals; whereas, in a premixed burner, the combustion products are not back mixed into the fuel and air. Lam *et al.* [4] reported that for an ethylene air flame at an equivalence ratio of 2.37, the soot concentration in the premixed burner at a height corresponding to 20 ms from the burner surface was eight times higher than for the WSR/PFR reactor sampled at 20 ms. The difference in mixing may also affect the size distribution. The soot inception region may terminate within the WSR so that only particle growth is occurring in the PFR section where the particles were sampled. The very low particle number concentrations observed at $\Phi = 1.9$ might be a result of the combustion of the early soot being back mixed into the air entering the WSR.

CONCLUSIONS

Soot size distributions were measured using a dilution probe followed by a Nano-DMA. A rapid insertion probe was fabricated to thermophoretically collect particles from the reactor for TEM analysis. Results were presented on the: (1) effect on the equivalence ratio of the soot size distributions obtained from the Nano-DMA for fixed dilution ratio (2) effect of dilution ratio on the soot size distributions obtained from the Nano-DMA for fixed equivalence ratio, and (3) comparison of soot size distributions obtained from the rapid insertion/TEM analysis and the Nano-DMA.

The difference in mixing conditions between a laminar premixed burner and a WSR resulted in either one or two peaks in the particle size distribution. A nucleation peak at the smallest particle size measured was observed with the premixed burner but not with the WSR. A comparison between the Nano-DMA results and the TEM results suggested that condensation was occurring during the rapid dilution process. Finally, these experiments have demonstrated that it was possible to use a gas cooled diluter in a combustion environment with temperatures of ≈ 1400 K.

ACKNOWLEDGEMENTS

This work was supported by the United States Department of Defense (DoD) through the Strategic Environmental Research and Development Program (SERDP). Mr. Charles Pellerin is the program manager. The assistance of Mr. Marco G. Fernandez with the experimental setup was crucial in performing the experiments and is greatly appreciated. Dr. Linda Blevins of Sandia National Laboratories is acknowledged for helpful discussions.

REFERENCES

1. Glassman, I., "Soot Formation in Combustion Process," *Proc. Comb. Inst.* 22: 295-311(1988).
2. Richter, H. and Howard, J.B. "Formation of Polycyclic Aromatic Hydrocarbons and their Growth to Soot-A Review of Chemical Reaction pathways," *Proc. Comb. Inst.* 26: 565-608 (2000).
3. Kennedy, I.M., "Models of Soot Formation and Oxidization," *Prog. Energy Combust. Sci.* 23, 95-132 (1997).
4. Lam, F.W., Longwell, J.P., and Howard, J.B., "The Behavior of Polycyclic Aromatic Hydrocarbons During the Early Stages of Soot Formation," *Proc. Comb. Inst.* 22:323-332 (1988).
5. Blevins, L.G., Jensen, K.A., Ristau, R.A., Yang, N.Y.C., Frayne, C.W., Striebich, R.C., DeWitt, M.J., Stouffer, S.D., Lee, E.J., Fletcher, R.A., Oran, J.M., Conny, J.M., Mulholland, G.W., "Soot Inception in a Well Stirred Reactor," 3rd Joint US Meeting of the Combustion Institute, Chicago, Illinois, March 2003.
6. Longwell J.P. and Weiss, M.A. (1955). "High Temperature Reaction Rates in Hydrocarbon Combustion." *Ind. Eng. Chem.* 47:1634-42.
7. Stouffer, S.D., Striebich, R.C., Frayne, C.W. and Zelina, J., "Combustion Particulates Mitigation Investigation Using a Well-Stirred Reactor," 38th Joint Propulsion Conference & Exhibit, 7-10 July 2002 Indianapolis, Indiana, AIAA 2002-37
8. Zhao, B., Yang, Z., Wang, J., Johnston, M.V., and Wang, H., "Analysis of Soot Nanoparticles in a Laminar Premixed Ethylene Flame by Scanning Mobility Particle Sizer", *Aerosol Sci. Tech.* 37:611-620 (2003).
9. Manzello, S.L., and Choi, M.Y., "Morphology of Soot Collected in Microgravity Droplet Flames", *Int. J. Heat Mass Trans.* 45:1109-1116 (2002).
10. Maricq, M.M., "Size and Charge of Soot Particles in Rich Premixed Ethylene Flames", *Combust. Flame* 37: 340-350 (2004).
11. Zhao, B., Yang, Z., Johnston, M.V., Wang, H., Wexler, A., Balthasar, M., and Kraft, M., "Measurement and numerical simulation of soot particle size distribution functions in a laminar premixed ethylene-oxygen-argon flame", *Combust. Flame* 133:173-188 (2003).